Journal of Materials Chemistry

Cite this: *J. Mater. Chem.*, 2011, **21**, 4346

www.rsc.org/materials

PAPER

Molecularly imprinted core-shell nanoparticles for determination of trace atrazine by reversible addition–fragmentation chain transfer surface imprinting

Shoufang Xu,[abc] Jinhua Li[ab] and Lingxin Chen*[ab]

Received 22nd October 2010, Accepted 10th January 2011
DOI: 10.1039/c0jm03593a

A simple and effective method was proposed to prepare uniform surface-imprinted nanoparticles. This strategy was carried out by introducing vinyl groups to the surface of silica beads by a one-step modification, followed by copolymerization of functional monomers *via* reversible addition–fragmentation chain transfer (RAFT) precipitation polymerization. Owing to the intrinsic advantages of controlled/living polymerization and surface imprinting technology, the resultant RAFT surface-imprinted nano-sized polymers (RAFT-SINPs) demonstrated spherical shaped particles with excellent monodispersity, and improvements in imprinting efficiency and mass transfer in comparison to molecularly imprinted polymers (MIPs) prepared by traditional precipitation polymerization. Recoveries of 93.4% and 79.8% were achieved by one-step extraction when RAFT-SINPs were used for the preconcentration and selective separation of atrazine in spiked corn and lettuce samples, respectively. These results provided the possibility for the separation and enrichment of atrazine from complicated matrices by RAFT-SINPs.

1 Introduction

Molecular imprinting is a versatile technique to create molecular recognition systems in three-dimensional cross-linked polymers, namely molecularly imprinted polymers (MIPs).[1–3] Thanks to the desired selectivity, physical robustness and thermal stability, MIPs have been widely applied as separation sorbents and recognition elements in sensors. To date, bulk polymerization is the commonly used method to prepare MIPs. However, extraction of original templates located at the interior area of bulk materials is quite difficult due to the high cross-linking nature of MIPs, which results in incomplete template removal, small binding capacity and slow mass transfer.[4] Several strategies, such as surface imprinting and nano-based imprinting techniques, have been proposed to overcome those limitations.

Surface imprinting, in which the imprinted templates are situated at the surface or in the proximity of the material's surface, is the most promising way to overcome those limitatons. Compared to traditional MIPs (TR-MIPs), surface imprinted polymers possess not only higher binding capacities but also faster mass transfer and binding kinetics, thanks to the complete template removal.[5]

Nano-based imprinting techniques are another way to help template removal. The main advantages recognized up to now in the use of nanomaterials arise from their characteristic large ratio of surface area to volume, which contributes to achieving favourable mass transfer rates. So, nano-based imprinting technology has been proposed for the purpose of the entire removal of templates. Molecularly imprinted nanospheres,[6,7] nanowires/nanotubes[8–10] and nanofilms[11,12] have been prepared in the past several years and they displayed superiority in the removal of templates and improved binding capacity.

Recent years have witnessed that reversible addition–fragmentation chain transfer (RAFT) is an ideal candidate for controlled/living free radical polymerization, due to its versatility and simplicity. RAFT polymerization has been used to prepare MIPs by surface imprinting for the determination of 2,4-dichlorophenoxyacetic acid[13] and L-phenylalanine anilide.[14] However, those procedures involved complex modification of core particles by immobilizing chain transfer agent (CTA) at the surface of the core particles.

In the present work, we proposed a novel and simple method to prepare atrazine-imprinted core-shell nanoparticles combining surface imprinting with nano-based imprinting technology and RAFT polymerization. Vinyl groups were first introduced to the surface of silica nanoparticles by a one-step modification, followed by copolymerization of functional

[a] *Yantai Institute of Coastal Zone Research, Chinese Academy of Sciences, Yantai, China. E-mail: lxchen@yic.ac.cn; Fax: +86-535-2109130; Tel: +86-535-2109130*
[b] *Key Laboratory of Coastal Zone Environmental Processes, CAS, Shandong Provincial Key Laboratory of Coastal Zone Environmental Processes, Yantai Institute of Coastal Zone Research, Chinese Academy of Sciences, Yantai, 264003, China*
[c] *Graduate University of Chinese Academy of Sciences, Beijing, 100049, China*

monomers with modified silica particles to prepare uniform imprinted polymers by RAFT precipitation polymerization. Compared to the MIPs prepared by traditional precipitation polymerization, the obtained RAFT surface-imprinted nano-sized polymers (RAFT-SINPs) showed spherical shaped morphology, higher binding capacity and faster mass transfer rates.

2 Experimental

2.1 Reagents

Tetraethylorthosilicate (TEOS) and γ-methacryloxypropyl trimethoxysilane (γ-MAPS) were purchased from Chemistry Reagent Factory of Chinese (Tianjing, China). Methacrylic acid (MAA), 4-vinylpyridine (4-VP), ethyleneglycol dimethacrylate (EGDMA), trimethylolpropane trimethacrylate (TRIM) and divinylbenzene (DVB) were purchased from Sigma-Aldrich and distilled in vacuum prior to use. 2,2′-azo-bis-isobutyronitrile (AIBN) were purchased from Shanghai Chemical Reagents Company and recrystallized in methanol prior to use. Acrylamide (AAm) was purchased from Tianjin Reagent Plant (Tianjin, China) and recrystallized in water prior to use. Atrazine, simetryn, propazine, ametryn were kindly provided by Binzhou Agricultural Technology Co. Ltd (Shandong, China). Furazolidone and carbendazim were purchased from J&K Technology Limited. The individual stock solutions (200 mg L^{-1}) were prepared in acetonitrile (ACN) and stored at −18 °C in the dark. High performance liquid chromatography (HPLC) grade acetonitrile was purchased from Merck (Darmstadt, Germany). HPLC water was doubly purified deionized water (18.2 MΩ cm specific resistance) obtained with a Pall Cascada laboratory water system. All other reagents were used as supplied without a further purification step.

2.2 Synthesis and modification of silica nanoparticles

Uniform silica particles were synthesized by hydrolysis of TEOS with aqueous ammonia, according to the reported Stöber method.[15] Subsequently, the monodisperse silica particles were chemically modified using γ-MAPS to introduce vinyl groups at the surface of silica beads, as previously reported.[16,17] Typically, 0.5 g of silica nanoparticles and 10 mL γ-MAPS were added into 50 mL of anhydrous toluene. The mixture was refluxed for 12 h under nitrogen atmosphere. The product was separated by centrifuge and washed with toluene, acetone and ether. Finally, the modified silica beads were dried under vacuum at 70 °C for 12 h.

2.3 Preparation of MIPs/NIPs

Uniform core-shell structured atrazine-imprinted polymers were prepared by RAFT precipitation polymerization, according to the non-covalent approach, using MAA as functional monomer, EGDMA as cross-linker and ACN as porogen. Briefly, prior to polymerization, pre-polymer solutions were prepared by dissolving MAA (0.35 mmol) and atrazine (0.0875 mmol) in ACN (50 mL), which were stored at 4 °C in dark for 12 h. Then, modified silica nanoparticles (30 mg), EGDMA (1.4 mmol), AIBN (10 mg), CTA (30 μL) were added. The solution was degassed in an ultrasonic bath for 5 min, then purged with nitrogen for 10 min while cooling in an ice bath for 10 min. Then, a two-step polymerization was carried out in a water bath at 50 °C for 8 h, followed by 24 h at 60 °C. The resultant polymer particles were separated and washed with methanol/acetic acid solution (9 : 1, v/v) to remove both the template molecules and residual monomers. Finally, the particles were dried to constant weight under vacuum at 40 °C. For comparison, surface imprinted nanoparticles were prepared by traditional precipitation polymerization in the same manner but without the addition of CTA (namely TR-SINPs). As a control, non-imprinted core-shell structured polymers were prepared by RAFT precipitation polymerization (NIPs) under identical conditions but omitting the template in the reaction system.

2.4 Characterization of MIPs

A FT-IR spectrometer (Thermo Nicolet Corporation, USA) was employed to examine the infrared spectra of samples using a pressed KBr tablet. The morphological evaluation was carried out by scanning electron micrography (SEM, JSM 5600 LV, operating at 20 kV). All samples were sputter-coated with gold before SEM analysis.

The adsorption experiments were carried out as follows: 20 mg of polymer nanoparticles were dispersed in a 5 mL flask containing 2.0 mL atrazine solutions of various concentrations. After shaking for 24 h at room temperature, the samples were centrifuged. The concentration of the supernatant solution was determined using HPLC. The amount of atrazine adsorbed onto the imprinted polymers was calculated by subtracting the amount of unbound compounds from the amount of compounds added to the mixture. Meanwhile, the binding kinetics were tested by monitoring the temporal amount of atrazine in the solutions at regular times. Selectivity experiments were carried out using simetryn, propazine, ametryn, furazolidone and carbendazim as structural analogs.

2.5 Analysis of atrazine in spiked samples

The edible parts of fresh lettuce and corn were taken and crushed into homogenates. 50 mL ACN was added into 50 g homogenate and incubated for 8 h before being filtered. The filtrate was extracted with dichloromethane and evaporated to dryness. The residue was redissolved in ACN. For spiked samples, appropriate amounts of atrazine standards were added into the ACN solution, at levels of 10 μg L^{-1}.

RAFT-SINPs of 80 mg were dispersed in 5 mL spiked solutions and incubated for 1 h at room temperature before being collected using a 0.22 μm microporous membrane. The RAFT-SINPs were washed with 3 mL methanol to reduce nonspecific adsorption, and then eluted with 1 × 5 mL desorption solvent (methanol/acetic acid, 9 : 1, v/v). The desorption solution was dried and redissolved in 200 μL ACN and then analyzed by HPLC. A C18 column with 250 mm × 4.6 mm i.d. was used as the analytical column. HPLC conditions employed for this work were as follows: mobile phase, acetonitrile/water (70 : 30, v/v); flow rate, 1.0 mL min^{-1}; room temperature; UV detection at 220 nm.

3 Results and discussion

3.1 Procedures of molecular imprinting at surface of silica nanoparticles

Surface imprinting is one of the most appealing ways to prepare MIPs with cavities at the surface or close to the surface, facilitating mass transfer. However, this procedure is still confronted with a severe challenge, that of issues of gelation due to the persistence of the initiator in solution. To overcome this problem, some appealing strategies, such as surface-bound free radical initiators[18,19] or chain transfer agents,[12] have been proposed. However, this procedure involved a complex surface modification process. Here, we present a simple method for preparing uniform surface-imprinted polymers. Fig. 1 illustrated the main steps involved in this surface imprinting procedure. In the first step, vinyl groups were introduced to the surface of silica nanoparticles through chemical modification with γ-MAPS for facilitating copolymerization with functional monomers. Then, the vinyl group-capped silica nanoparticles were suspended in ACN solution containing functional monomer (MAA), cross-linker (EGDMA), template (atrazine), chain transfer agent (CTA) and initiator (AIBN). After RAFT precipitation polymerization at 50 °C for 6 h, followed by 60 °C for 24 h, a uniform molecular imprinting layer was coated at the surface of silica particles. Finally, recognition sites located at the surface of the obtained MIPs were shaped after the removal of the template molecules. Compared to the complex surface modification for immobilized CTA, the procedures proposed in this work were simple and easy to control. In this method, two kinds of strategies were used in order to form a uniform shell. One is the two-step-temperature polymerization method. In the first polymerization stage at lower temperature, polymerization proceeds slowly, and then a thin oligomer layer can form at the surface of silica particles, which induced the following polymerization to occur at the surface of the silica nanoparticle. The shell was mainly shaped during the second process at higher temperature with faster polymerization. The second strategy used in this work was controlled/living free radical polymerization, which can adjust the polymerization velocity and polymer structure. Combining the two methods, uniform core-shell structured surface-imprinted nanoparticles were prepared.

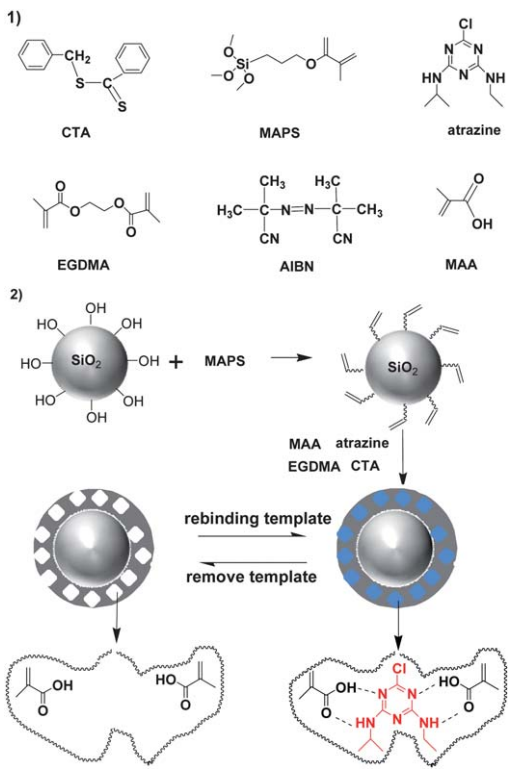

Fig. 1 Structures of chemicals used in this study (1) and a schematic of the preparation of atrazine-imprinted core-shell nanopolymers by RAFT precipitation polymerization (2).

3.2 Preparation and characterization of vinyl group-capped silica nanoparticles

Uniform silica nanoparticles with diameters of 180 nm were prepared by hydrolysis of TEOS with aqueous ammonia using a single-step process. Vinyl groups were introduced to the surface of the silica nanoparticles by immobilized γ-MAPS onto the surface of silica nanoparticles for subsequent copolymerization with functional monomers in the solution phase. The colour of those silica nanoparticles changed from white to faint yellow after surface modification with vinyl groups. The faint yellow particles obtained were further characterized by infrared spectra. Fig. 2 shows the infrared spectra of pure silica (a) and vinyl group-modified silica nanoparticles (b). Compared with the infrared spectrum of pure silica, the vinyl group-modified silica nanoparticles displayed the characteristic peaks of carbonyl groups at 1728 cm^{-1}, as indicated by the arrow in Fig. 2. This result indicated that vinyl groups have been successfully introduced to the surface of the silica nanoparticles. Fig. 3 shows the SEM images of silica and vinyl group-modified silica nanoparticles. Compared with pure silica nanoparticles, the modified silica particles are still monodisperse, with highly smooth surfaces.

3.3 Optimization of surface-imprinting synthesis conditions

It is well known that the functional monomer, cross-linker and porogen have a profound impact on the morphology and binding capacity of MIPs, so the functional monomers (MAA, AAm and

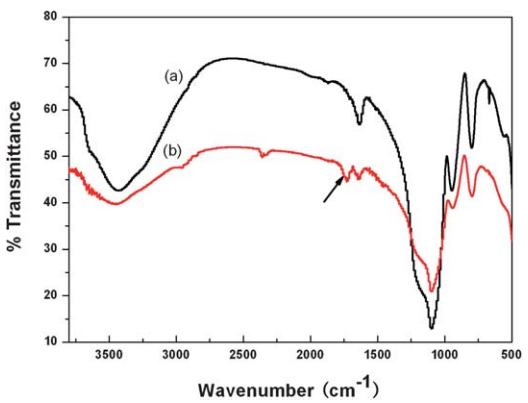

Fig. 2 FTIR spectra of SiO_2 (a) and vinyl group-modified SiO_2 (b).

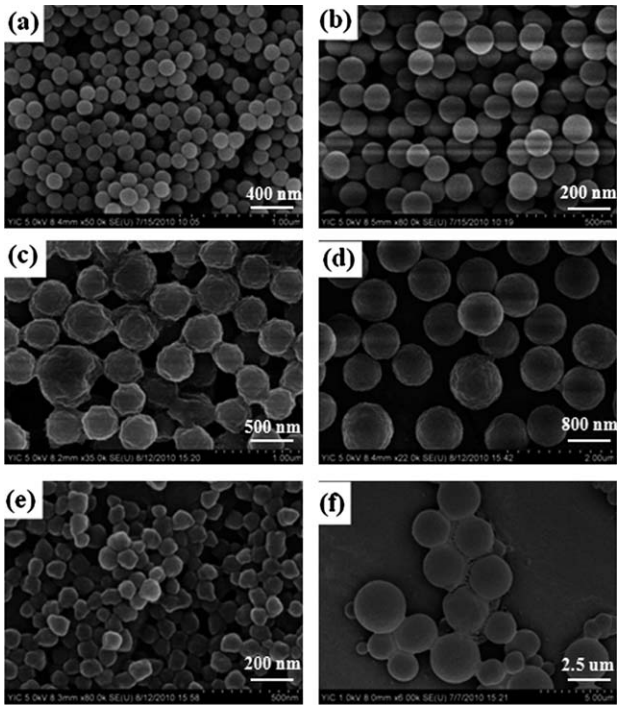

Fig. 3 The SEM microphotographs of pure silica particles (a), vinyl group-modified silica particles (b), atrazine-imprinted nanoparticles prepared by traditional precipitation polymerization with 0.3 g polymerization precursors (c), atrazine-imprinted nanoparticles prepared by RAFT precipitation polymerization with 0.4 g polymerization precursors (d), atrazine-imprinted polymer particles prepared using pure silica nanoparticles (e) and atrazine-imprinted polymers with 100 mg modified silica nanoparticles (f).

4-VP), cross-linkers (EGDMA, TRIM and DVB) and porogens (ACN, toluene and chloroform) were optimized. Finally, MAA, EGDMA and ACN were chosen to prepare atrazine-imprinted polymers. In addition to the commonly considered factors, the amount of polymerization precursors, including functional monomers and cross-linkers, used in polymerization should be investigated because the correct shell thickness was critical to achieve the maximum binding capacity. Low amounts of polymerization precursors lead to thinner shells, which is beneficial for complete template removal, thereby improving the accessibility of the binding sites and reducing the mass transfer resistance, allowing all of the recognition sites to be used. However, the silica core does not contribute to template binding, which results in a lower binding capacity per unit mass of MIPs. On the contrary, a thicker shell layer would result in incomplete template removal and aggregation of imprinted nanoparticles, just like the traditional MIPs. In the present work, 40 mg silica nanoparticles were dispersed in 50 mL ACN. The thickness of the shell layer can be adjusted from 150 nm to 350 nm by changing the amount of polymerization precursors from 0.2 g to 0.5 g (the mole ratio of functional monomer to cross-linker is consistently 1 : 4). Maximum binding capacity was obtained when 0.4 g of polymerization precursor was used, while the shell layer thickness was about 300 nm. Further increasing the polymerization precursors would result in homogeneous self-polymerization of monomers. Keeping the amount of polymerization precursors constant (0.4 g), the aggregation of imprinted polymers became more and more serious on increasing the amount of silica beads from 40 mg to 100 mg, because the silica particles were inclined to aggregate in the organic solvent. So, in this work, the optimized shell layer thickness of 300 nm was obtained when 0.4 g polymerization precursors and 40 mg silica nanoparticles were used, as can be seen in Fig. 2(d).

3.4 Characterization of atrazine-imprinted core-shell nanoparticles

Scanning electron micrography. SEM was employed to observe the morphology of the pure silica particles, modified silica particles, atrazine surface-imprinted nanopolymers and surface non-imprinted polymers (NIPs) (Fig. 3). Pure silica particles and vinyl group-modified silica particles showed spherical shapes and smooth surfaces, as can be seen from Fig. 3(a) and (b). Fig. 3(c) and (d) show the atrazine-imprinted nanoparticles at the surface of vinyl group-modified silica beads prepared by traditional precipitation polymerization (TR-SINPs) and RAFT precipitation polymerization (RAFT-SINPs), respectively. It can be clearly seen that RAFT-SINPs kept the spherical shape with favourable monodispersity when 0.4 g polymerization precursor was used (Fig. 3d). However, under the same conditions TR-SINPs inter-adhered. Even if a small quantity of polymerization precursor (0.3 g) was used, the adhesion of the polymers could not be avoided (Fig. 3c). This feature could be attributed to the intrinsic characteristics of the controlled/living polymerization mechanism of RAFT precipitation polymerization. Ascribed to the mechanism of traditional free radical polymerization, the microstructure, degree of polymerization, and polydispersity of the obtained polymers are uncontrollable. The existence of irreversible chain transfer reactions resulted in the aggregation of polymer particles. Thanks to the intrinsic advantages of "living" polymerization in the RAFT polymerization process, the lifetime of the growing radical can be controlled, resulting in the synthesis of polymer chains with pre-defined molar masses, low polydispersity and controlled composition, yielding RAFT-SINPs with uniform and spherical particle morphology. As can be seen in Fig. 3(e), when pure silica nanoparticles were used as core materials, the homogeneous self-polymerization of monomers in solution phase was unavoidable, and secondary particles with size of 100 nm were formed in solution. The result indicated that vinyl group surface modification is necessary in order to induce polymerization occurring at the surface of silica particles. When more core particles were used in surface imprinting, silica nanoparticles could not monodisperse in the polymerization solution, which resulted in the aggregation of silica particles. Imprinted polymers encase the aggregated silica particles to form large bulk polymers, as seen in Fig. 3(f). The SEM results indicated that vinyl group modification of silica nanoparticles and RAFT polymerization were two important conditions for the surface imprinting process.

Binding experiments. In order to investigate the binding performance of the RAFT-SINPs, an equilibrium binding analysis was carried out using atrazine in the concentration range 10–50 mg L^{-1}. Fig. 4 showed that RAFT-SINPs have the highest binding capacity compared to the control polymers, and

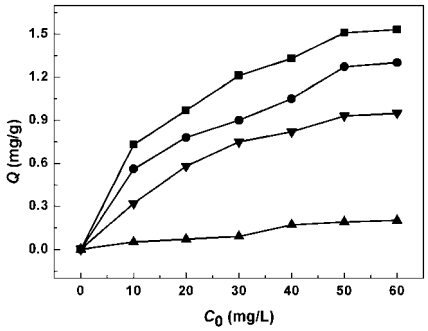

Fig. 4 Binding isotherm of MIPs and NIPs for atrazine in acetonitrile. (■ RAFT-SINPs; ● TR-SINPs; ▼ TR-MIPs; ▲ RAFT-NIPs;). Experimental conditions: V = 2.0 mL; the mass of polymer, 20 mg; adsorption time, 24 h.

benefited from their excellent monodispersity and the intrinsic advantages of controlled/living polymerization. The binding capacity of both RAFT-SINPs and TR-SINPs were higher than the MIPs prepared by commonly-used precipitation polymerization (TR-MIPs, with the size of 3 μm), which can be attributed to the advantages of nano-materials. Nano-structured imprinted materials have high surface-to-volume ratios, so most of the template molecules are situated at the surface. Thus, the extraction of the original templates is quite convenient and recognition sites can be utilized completely. There were no specific recognition sites in the NIPs, so the binding capacity of NIPs was the lowest.

The Scatchard equation was employed to evaluate the maximum binding capacity of the MIPs.[20] The Scatchard equation is expressed as:

$$\frac{Q}{C_e} = \frac{Q_{\max}}{K_d} - \frac{Q}{K_d}$$

where Q stands for the binding capacity (mg g^{-1}) of atrazine on polymers, K_d represents the equilibrium dissociation constant (mg L^{-1}), Q_{max} (mg g^{-1}) is the theoretical maximum adsorption amount of template molecules on polymers, and C_e (mg mL^{-1}) is the equilibrium concentration of atrazine in the solution. The maximum binding capacities for RAFT-SINPs, TR-SINPs, and TR-MIPs were 1.92 mg g^{-1}, 1.80 mg g^{-1} and 1.53 mg g^{-1}, respectively. The result was in correspondence with the binding experiment.

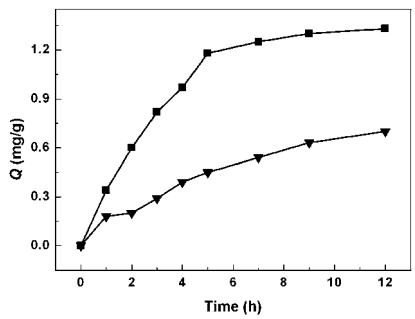

Fig. 5 Kinetic uptake of atrazine molecules onto RAFT-SINPs (■) and TR-MIPs (▼). Experimental conditions: V = 2.0 mL; C_0 = 40 mg L^{-1}; the mass of polymer, 20 mg.

The binding kinetics of the RAFT-SINPs and TR-MIPs were evaluated. It can be seen from Fig. 5 that RAFT-SINPs exhibited a much higher binding capacity and faster mass transfer rate than TR-MIPs. For RAFT-SINPs, the adsorption capacity increased faster in the first 5 h and reached equilibrium within 7 h. For TR-MIPs, the equilibrium time was 12 h. This phenomenon can be explained as follows: combining the advantages of surface-imprinted polymers with nano-sized MIPs, most recognition sites are situated at the surface of the RAFT-SINPs, which facilitates the mass transfer. So, the forms of surface-imprinted nano-materials are expected to improve the binding capacity, kinetics and site accessibility.[21]

To further evaluate the specificity of the RAFT-SINPs, an adsorption specificity experiment was carried out for the binding of ametryn, propazine, simetryn and atrazine, and two references (furazolidone and carbendazim) as other herbicides, whose structures are shown in Fig. 6. The binding of these compounds was investigated by equilibrium binding experiments at an initial concentration of 40 mg L^{-1}. It can be seem from Fig. 6 that RAFT-SINPs exhibited good adsorption selectivity for the template molecule. The adsorption capacity for atrazine was much higher than the structural analogs. Although the same hydrogen bond can form between the structural analogs and the functional monomers, because of the similar structure to the template molecule, the adsorption capacity was much lower than for the template molecule. This result shows the recognition mechanism of MIPs, which is based on the interaction of size, shape, and functionality to the template.[22] For NIPs, there was

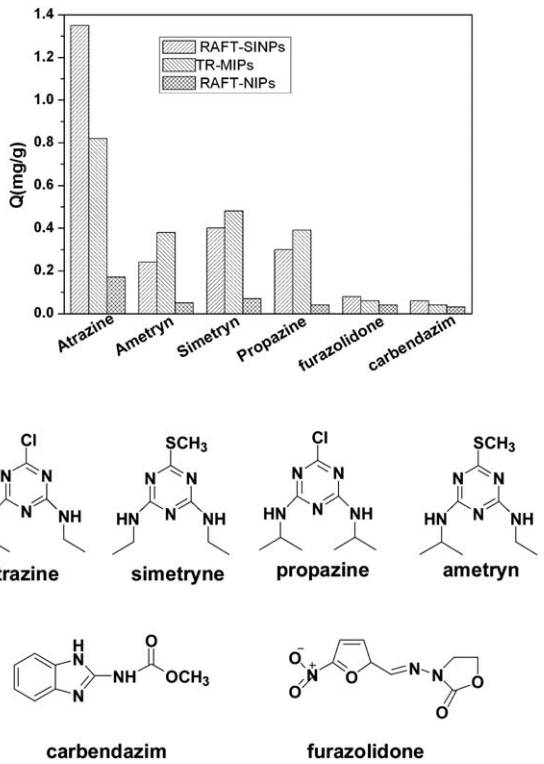

Fig. 6 Selectivity of MIPs and NIPs for atrazine, ametryn, propazine and simetryn. The conditions for the measurements were as follows: polymer, 20 mg; initial concentration of the compounds, 40 mg L^{-1}; V = 2.0 mL; adsorption time, 24 h; room temperature.

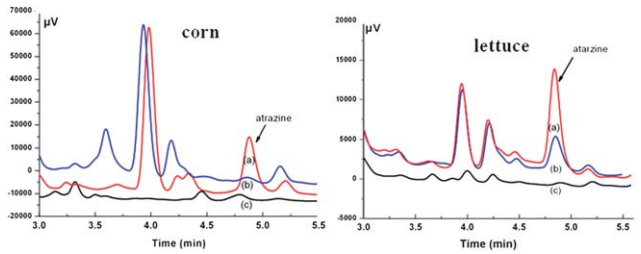

Fig. 7 HPLC chromatograms of spiked corn and lettuce samples. (a) extracted with RAFT-SINPs; (b) extracted with NIPs; (c) spiked solution containing 10 μg L^{-1} atrazine. Experimental conditions: 5 mL spiked solutions; 80 mg RAFT-SINPs; wash solution, 3 mL methanol; eluent solution, 5 mL methanol/acetic acid, 9 : 1, v/v; re-dissolve solution, 200 μL ACN. HPLC conditions: mobile phase, acetonitrile/water (70 : 30, v/v); flow rate, 1.0 mL min^{-1}; room temperature; UV detection, at 220 nm.

no tailor-made recognition site formed in those polymers, so NIPs bind the test compounds only by non-specific adsorption. As a result, NIPs adsorbed the template molecules much less than the MIPs, and there was no significant difference in binding capacity for the competitive compounds.

3.5 Selective separation of atrazine from the spiked samples

To evaluate the application of RAFT-SINPs to selective separation of atrazine, the lettuce and corn samples spiked with atrazine at 10 μg L^{-1} were analyzed (Fig. 7), while NIPs and traditional C18 column separation were used for comparison. As can be clearly seen from Fig. 7(c), no atrazine was detected in spiked corn and lettuce samples because of low concentrations. The peak of atrazine sharply increased after extraction by RAFT-SINPs (Fig. 7(a)). NIPs did not show a selectively enriched ability for atrazine binding because no specific binding sites exist on them, so only a small quantity of atrazine was detected after extraction by NIPs (Fig. 7(b)). Under the same conditions, no signal can be detected for atrazine when the C18 column was used. Therefore, higher sensitivity can be achieved by using RAFT-MIPs as the extraction sorbent. Furthermore, recoveries of 93.4% and 79.8%, with the RSD of 1.8% and 5.7% were obtained for the corn and lettuce spiked samples, respectively. The results demonstrated that RAFT-SINPs had high selectivity and enrichment ability. Hence, the RAFT-SINPs offer a simple and straightforward technique for direct analysis of atrazine from complicated vegetable samples.

Conclusions

A simple and effective method was developed to prepare silica surface-imprinted nanoparticles with uniform morphology and controllable layer thickness by introducing vinyl groups to the surface of silica beads followed by copolymerization of the silica with functional monomers *via* RAFT precipitation polymerization. The resultant RAFT-SINPs show some attractive characteristics, such as uniform morphology, higher binding capacity and quicker mass transfer. The analytical method based on RAFT-SINPs was successfully applied to atrazine analysis in spiked lettuce and corn samples with higher selectivity and sensitivity. The approach proposed herein provides an opportunity for imprinting various molecules in a simple way and forms the basis of selective separation and fast enrichment of atrazine from complicated matrices.

Acknowledgements

Financial support from the Department of Science and Technology of Shandong Province of China (2008GG20005005), the National Natural Science Foundation of China (20975089), the Chinese Academy of Sciences (KZCX2-EW-206), the 100 Talents Program of the Chinese Academy of Sciences, and the Department of Science and Technology of Yantai City of China (2010158) is gratefully acknowledged.

Notes and references

1 J. Fan, Y. Wei, J. Wang, C. Wu and H. Shi, *Anal. Chim. Acta*, 2009, **639**, 42–50.
2 H. Yan, K. H. Row and G. Yang, *Talanta*, 2008, **75**, 227–232.
3 X. Song, J. Li, J. Wang and L. Chen, *Talanta*, 2009, **80**, 694–702.
4 S. C. Zimmerman and N. G. Lemcoff, *Chem. Commun.*, 2004, 5–14.
5 D. Gao, Z. Zhang, M. Wu, C. Xie, G. Guan and D. Wang, *J. Am. Chem. Soc.*, 2007, **129**, 7859–7866.
6 F. Priego-Capote, L. Ye, S. Shakil, S. A. Shamsi and S. Nilsson, *Anal. Chem.*, 2008, **80**, 2881–2887.
7 Z. Li, J. Ding, M. Day and Y. Tao, *Macromolecules*, 2006, **39**, 2629–2636.
8 H. Yang, S. Zhang, F. Tan, Z. Zhuang and X. Wang, *J. Am. Chem. Soc.*, 2005, **127**, 1378–1379.
9 H. Wang, W. Zhou, X. Yin, Z. Zhuang, H. Yang and X. Wang, *J. Am. Chem. Soc.*, 2006, **128**, 5954–15955.
10 C. Xie, B. Liu, Z. Wang, D. Gao, G. Guan and Z. Zhang, *Anal. Chem.*, 2008, **80**, 437–443.
11 M. Riskin, R. Tel-Vered and I. Willner, *Adv. Funct. Mater.*, 2007, **17**, 3858–3863.
12 F. Shi, Z. Liu, G. Wu, M. Zhang, H. Chen, Z. Wang, X. Zhang and I. Willner, *Adv. Funct. Mater.*, 2007, **17**, 1821–1827.
13 C. Lu, W. Zhou, B. Han, H. Yang, X. Chen and X. Wang, *Anal. Chem.*, 2007, **79**, 5457–5461.
14 M. M. Titirici and B. Sellergren, *Chem. Mater.*, 2006, **18**, 1773–1779.
15 W. Stöber, A. Finker and E. Bohn, *J. Colloid Interface Sci.*, 1968, **26**, 62–69.
16 W. Zhang, L. Qin, X. He, W. Li and Y. Zhang, *J. Chromatogr., A*, 2009, **1216**, 4560–4567.
17 Q. Lu, X. Chen, L. Nie, J. Luo, H. Jiang, L. Chen, Q. Hu, S. Du and Z. Zhang, *Talanta*, 2010, **81**, 959–966.
18 L. Qin, X. He, W. Zhang, W. Li and Y. Zhang, *J. Chromatogr., A*, 2009, **1216**, 807–814.
19 C. Sulitzky, B. Rückert, A. J. Hall, F. Lanza, K. Unger and B. Sellergren, *Macromolecules*, 2002, **35**, 79–91.
20 J. Fan, Y. Wei, J. Wang, C. Wu and H. Shi, *Anal. Chim. Acta*, 2009, **639**, 42–50.
21 G. Guan, B. Liu, Z. Wang and Z. Zhang, *Sensors*, 2008, **8**, 8291–8320.
22 Y. Chang, T. Ko, T. Hsu and M. Syu, *Anal. Chem.*, 2009, **81**, 2098–2105.